

# Design of Light Weight Microstrip Patch Antenna on Dielectric and Magnetodielectric Substrate for Broadband Applications in X-Band

Kunal Borah<sup>1</sup>, Arunav Phukan<sup>1</sup>,  
Satyajib Bhattacharyya<sup>2</sup>, and Nidhi Saxena Bhattacharyya<sup>1, \*</sup>

**Abstract**—A modification in the structure of a substrate has been carried out to reduce weight and improve the performance of microstrip patch antenna in X-band. A step profile is incorporated in the substrate along the radiating edges of the patch. The design is tested on both dielectric and magnetodielectric substrates. Return loss of antenna with varying step riser height and step tread length shows improvement in  $-10$  dB bandwidth to 13.2% for the dielectric and to 12.3% for the magnetodielectric as compared to about 4.8% and 6.9% for unprofiled substrate geometry in dielectric and magnetodielectric respectively. As compared to the unprofiled planar antenna, maximum weight reduction for the stepped antenna on dielectric substrate is 54.75 % and for the magnetodielectric is 58.9% is observed. An equivalent circuit modeling for the stepped structure is carried out for the proposed structure.

## 1. INTRODUCTION

Present day communication systems require portable and light weight devices, and hence weight reduction of antenna is a major design challenge for practical applications. In addition, high-speed data communication systems at high-frequency demands for broadband antennas. Printed antennas are economical and easily hidden inside packages, making them well suited for consumer applications. Unfortunately, a “classical” microstrip printed antenna has a very narrow frequency bandwidth that precludes its use in typical communication systems. A few approaches to improve the microstrip antenna bandwidth [1] includes increasing the substrate thickness, introducing parasitic element either in coplanar or stack configuration, and modifying the shape of a common radiator patch by incorporating slots and stubs [2]. The bandwidth of microstrip antenna can be increased by using air as substrate [3], but this may lead to bulky antennas and hence, inconvenient to use. Usually dielectric substrates are used to make antennas compact [4], but whenever the substrate permittivity  $\epsilon_r > 1$  surface waves get excited on microstrip antenna, degrading its performance.

Several methods have been used to overcome these drawbacks by manipulating the antenna substrate geometry. Jackson et al. [5] eliminated excitation of  $TM_0$  surface waves by designing a ring of magnetic current of particular radius in the substrate. Other suggested approaches are to lower the effective dielectric constant of the substrate by replacing the substrate with air and suspending the patch antennas by dielectric posts [6, 7]. Designing patch on electromagnetic band-gap structure [8, 9] is reported to reduce the surface waves and improve performance. In [10] lowering of effective dielectric constant of substrate is carried out by replacing completely the substrate surrounding the patch by air.

Here, the effective dielectric constant is lowered by partially etching the substrate laterally along the radiating edge. The study of antenna performance is made by varying step riser height and step tread length. An equivalent circuit model (ECM) is developed for the stepped substrate geometry and performance verified with the measured data.

---

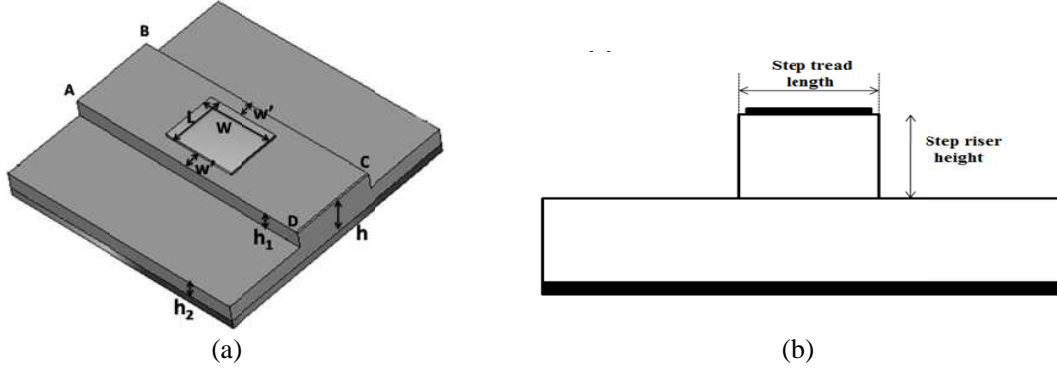
Received 1 May 2014, Accepted 19 June 2014, Scheduled 29 June 2014

\* Corresponding author: Nidhi Saxena Bhattacharyya (nidhisbhatta@gmail.com).

<sup>1</sup> Microwave Engineering Laboratory, Department of Physics, Tezpur University, Napaam, Tezpur, Assam 784028, India. <sup>2</sup> Microwave Research Laboratory, Department of ECE, Tezpur University, Napaam, Tezpur, Assam 784028, India.

**Table 1.** Patch dimension for the different substrate materials.

	5% VF nickel ferrite/LDPE magnetodielectric substrate	Dielectric glass epoxy
Length of patch ( $L$ )	6.41 mm	8.1 mm
Width of patch ( $W$ )	9.20 mm	11.5 mm

**Figure 1.** (a) Schematic of the step profile antenna. (b) Schematic with terminology.

## 2. DESIGN AND FABRICATION OF STEP PROFILED SUBSTRATE ANTENNA

The MPA at 8 GHz is fabricated on (3 cm × 3 cm) dielectric glass epoxy ( $\epsilon_r = 4.3$ ,  $\mu_r = 1$  and  $h = 2$  mm) and on synthesized (3 cm × 3 cm) 5% VF nickel ferrite /LDPE magnetodielectric substrate ( $\epsilon_r = 7.3$ ,  $\mu_r = 1.3$  and  $h = 2$  mm) [11] using transmission line modeling (TLM). Table 1 shows the dimensions of the radiating patch for the two substrate materials.

Step profile on glass epoxy is designed by gradually grinding the lateral parts along the radiating edges. A grinding machine of least count 0.01 mm with an attachment of 12 mm diameter is used for the purpose. The antenna is held tightly with a metallic holder, and the lateral parts are grinded slowly keeping the movement in one direction. An elevated segment,  $ABCD$  or stepped region, as shown in Figure 1(a) is obtained. While for 5% VF nickel ferrite /LDPE composite, the substrate is prepared by using a mould of the required dimension and shape. The nickel ferrite/LDPE composite mixture is placed in a specially designed step mould with a provision for variation in the step riser height and step tread length. The sample is initially heated up to 80°C and then allowed to cool at room temperature.

A schematic diagram of the stepped design is shown in Figure 1(b). MPA with three step riser height variations,  $h_1 (= h - h_2)$ , of 0.5 mm, 1 mm and 1.5 mm for EP1, EP2 and EP3, respectively, is fabricated with width  $w' \approx 0$ , where,  $w'$ , is length beyond the radiator edge.

Further, tread length (total step tread length  $L + 2w'$ ) variation is done by changing  $w'$ , such that  $w' \geq L$ , where,  $L$  is the length correction factor due to fringing fields. Three configurations EP4, EP5 and EP6 with  $w'$  as 0.5 mm, 0.75 mm and 1 mm, respectively, is designed with the riser height,  $h_1 = 1.5$  mm ( $h_1$  is chosen on the basis of the best return loss results).

Step profiling of MPA is done with the same variations of step riser height and step tread length for both glass epoxy and the nickel ferrite substrate. Hence, the kept same for both the cases.

## 3. EQUIVALENT CIRCUIT MODELING OF THE STEP PROFILE PATCH ANTENNA

An equivalent circuit model is developed for the stepped structure. The microstrip antenna on the proposed structure is approximated as two regions: *region I*, the area (shown in dashed lines) beneath the patch and between the ground and *region II*, the area (shown in dotted lines) in close proximity to the radiating edges of the patch, as shown in Figure 2.

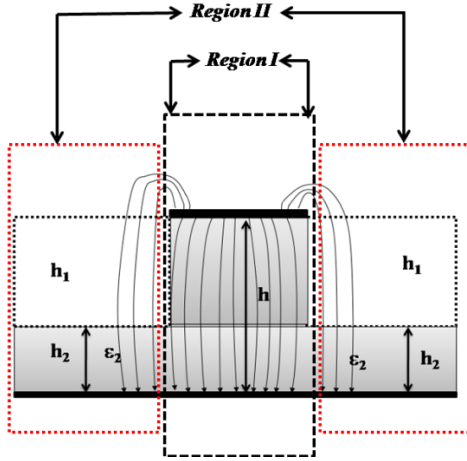


**Figure 2.** Schematic showing field lines for step profile antenna.

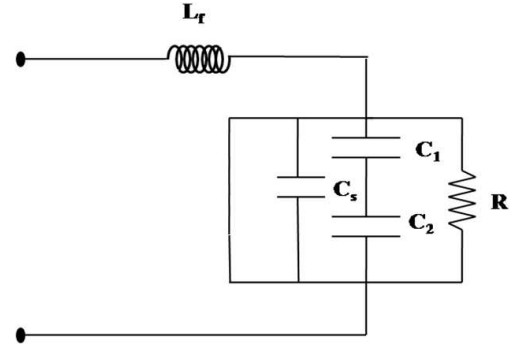


**Figure 3.** Equivalent circuit model of the step profiled antenna structure on dielectric substrate.

In *region I*, the line capacitance,  $C_s$ , is entirely due to the electric field within the substrate with relative permittivity,  $\epsilon_r^{sub}$ , sandwiched between the patch and the ground plane. The *region II*, can be considered as two layer structure, with one layer as air ( $\epsilon_r^{air} = 1$ ) and the other as the substrate, with the fringing electric field partially traversing through air and then the substrate. Figure 3 shows the equivalent circuit model. If  $C_1$  and  $C_2$  are capacitance due to air and substrate, respectively, then, the fringing field capacitance,  $C_f$ , for the entire *region II*, can be considered as series combination of the two capacitances and given by expression,

$$\frac{1}{C_f} = \frac{1}{C_1} + \frac{1}{C_2} \quad (1)$$

The total capacitance of the *region I* and *II*,  $C_{total}$ , can be expressed as

$$C_{total} = C_s + C_f \quad (2)$$

As the substrate is laterally etched, in the *region II*, the fringing field will travel more in air than in the substrate and this will affect  $C_f$  [12] and hence,  $C_{total}$ . The associated equivalent permittivity of the two layered structure with air of thickness,  $h_1$ , and the substrate of height,  $h_2$ , can be calculated from the fringing field capacitance

$$\epsilon_{eq}^f = \frac{h\epsilon_r^{sub}\epsilon_r^{air}}{h_2\epsilon_r^{air} + h_1\epsilon_r^{sub}} \quad (3)$$

where, total height of the region,  $h = h_1 + h_2$ .

The total equivalent permittivity for the entire structure from Equation (2) is,

$$\epsilon_{eq}^{total} = \epsilon_{eq}^f + \epsilon_r^{sub} \quad (4)$$

Using two conformal mapping functions, the area of interest can be transformed into a rectangle [13, 14]. Since capacitance is invariant with the transformation of coordinates, the effective permittivity of the stepped structure can be given as,

$$\epsilon_{eff} = 1 + 2 \left( \epsilon_{eq}^{total} - 1 \right) K_{air}'(k) \frac{K'(k)}{K(k)} \quad (5)$$

where,  $K(k)$ , is the complete elliptical integral of the first kind,  $k' = \sqrt{1 - k^2}$ , and  $k$  is the wave number.  $k(air) = \epsilon_0 v_p Z_0^{air}$ , where,  $v_p$ , is the phase velocity and  $Z_0^{air}$ , is the free space impedance.

The ratio of complete elliptical integral of the first kind can be approximated as,

$$\frac{K'(k)}{K(k)} \approx \frac{\pi}{2 \ln 2 + \left( \frac{\pi w}{4h_1} \right)} \quad (6)$$

For the step profile designed on magnetodielectric substrate, an additional line inductance  $L$  is attached parallel with the line capacitance as shown in Figure 4.

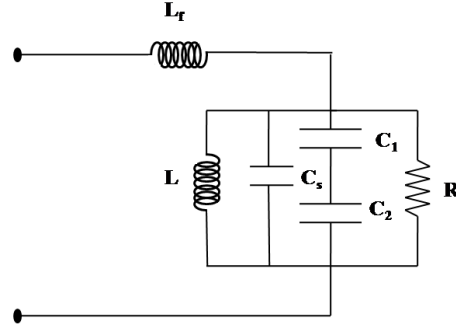


**Figure 4.** Transmission line equivalent circuit model of the proposed step structure on magnetodielectric substrate.

Analogous to effective permittivity, an effective permeability parameter is considered for field lines traveling partially through air and magnetodielectric material along the radiating edge of the MPA. The effective permeability can be calculated using [15]

$$\epsilon_{eff} \frac{1}{\mu_{eff}} \quad (7)$$

Lateral etching of the substrate in *region II*, changes the line inductance leading to change in the effective permeability of the substrate.

Putting (7) in (5),

$$\mu_q^{total} = \frac{\mu_{eq}^f + \mu^s}{\mu_{eq}^f \mu^s} \quad (8)$$

Thus,

$$\mu_{eff} = \frac{1}{1 + 2 \left[ \frac{\mu_{eq}^f + \mu^s}{\mu_{eq}^f \mu^s} - 1 \right] k_{air} \frac{K'(k)}{K(k)}} \quad (9)$$

$\epsilon_{eff}$  and  $\mu_{eff}$  expressions are used later to analyze the results with step raiser height variation.

#### 4. ANTENNA PERFORMANCE MEASUREMENTS

The  $S_{11}$  measurements are carried out using E8362C vector network analyzer over the X band. The  $E$  and  $H$  plane radiation pattern measurements are carried out using an automated measurement setup with a PC (personal computer) controlled turn table. The system is calibrated using two standard horn antennas at receiving and transmitting ends. The radiation pattern measurements are taken in open space to avoid reflections of microwave signals from the walls in laboratory.

##### 4.1. Results for Step Profile Antenna on Dielectric Substrate

$S_{11}$  parameter and radiation pattern studies are conducted on the step profiled MPA using standard glass epoxy substrate over the X-band, with variation in the step riser height and tread length of the stepped region.

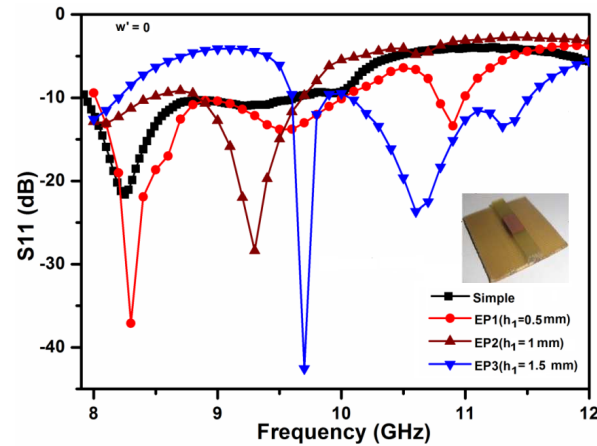


**Figure 5.**  $S_{11}$  (measured) of the step profile antenna for different step riser heights on glass epoxy substrate.

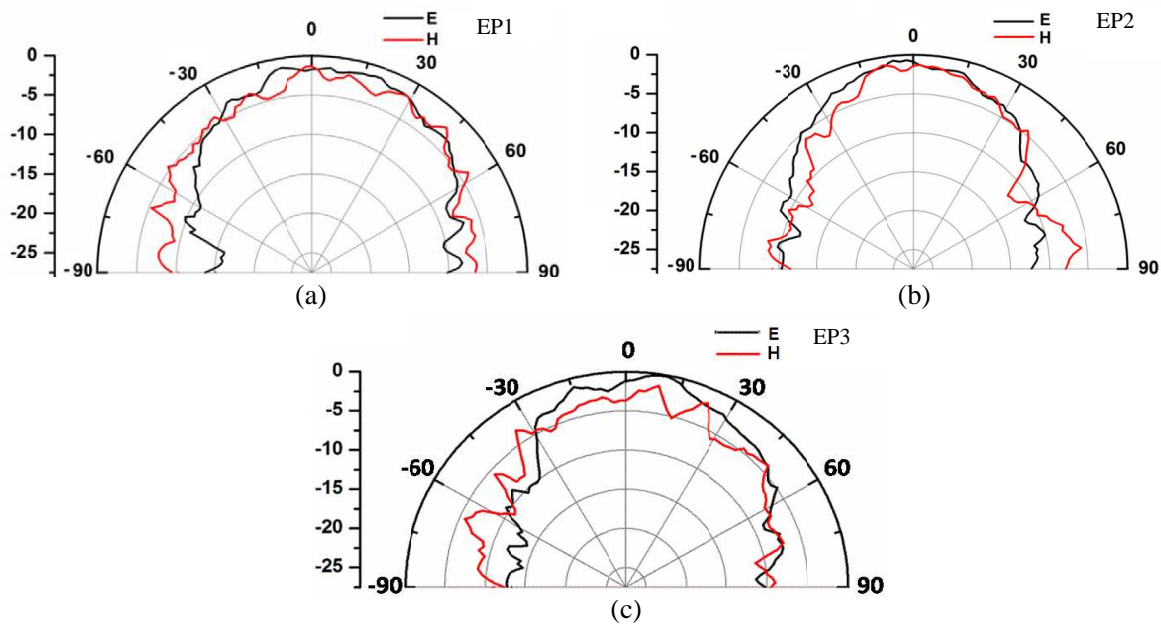


**Figure 6.** (a)  $E$  and  $H$  plane radiation patterns (measured) of EP1 ( $h_1 = 0.5$  mm) on glass epoxy substrate. (b)  $E$  and  $H$  plane radiation patterns (measured) of EP2 ( $h_1 = 1$  mm) on glass epoxy substrate. (c)  $E$  and  $H$  plane radiation patterns (measured) of EP3 ( $h_1 = 1.5$  mm) on glass epoxy substrate.

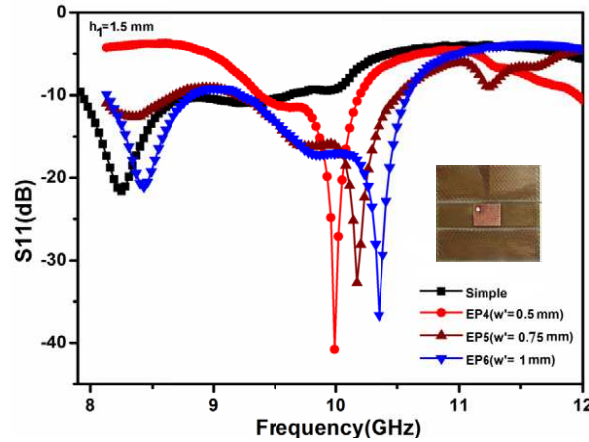
#### 4.1.1. Performance Study with Step Riser Height

Figure 5 shows  $S_{11}$  plots with step riser height variations in case of glass epoxy substrate. EP3 shows maximum shift of  $\sim 1.8$  GHz from the planar patch resonant frequency with  $-10$  dB bandwidth of 2.9%, while, EP1, shows the least shift.  $S_{11}$  increases with step riser height. The results are tabulated in Table 2.

The measured radiation patterns in both  $E$  and  $H$  planes for  $h_1 = 0.5$  mm, 1 mm and 1.5 mm are shown in Figures 6(a), (b) and (c), respectively. The directivities are tabulated in Table 2.

**Table 2.** Different measured parameters for MPA on nickel ferrite/LDPE substrate and dielectric substrate for varying step riser height and step tread length.

MPA type	Step riser height variation							
	Glass Epoxy				5% VF nickel ferrite/LDPE			
	$f_r$ (GHz)	$S_{11}$ (dB)	-10 dB Bandwidth	$D$ (dBi)	$f_r$ (GHz)	$S_{11}$ (dB)	-10 dB Bandwidth	$D$ (dBi)
Planar	8.2	-17.38	4.8%	10.96	8.5	-30.16	6.9%	9.91
EP1	8.296	-37.08	11.19%	11.05	8.5	-29	2%	8.54
EP2	9.30	-28.31	10.5%	10.83	9.4	-38.31	8.5%	8.25
EP3	9.71	-42	2.9%	11.34	10.25	-40.47	12.3%	8.63
MPA type	Step tread length							
	Glass Epoxy				5% VF nickel ferrite/LDPE			
	$f_r$ (GHz)	$S_{11}$ (dB)	-10 dB Bandwidth	$D$ (dBi)	$f_r$ (GHz)	$S_{11}$ (dB)	-10 dB Bandwidth	$D$ (dBi)
EP4	9.99	-40.89	8.2%	10.47	9.90	-30	2.7%	9.21
EP5	10.17	-32.78	12.9%	11.59	9.95	-36.2	10%	8.05
EP6	10.34	-36.5	13.2%	14.14	10.3	-39.6	11.6%	8.36



**Figure 7.**  $S_{11}$  (measured) of the step profile antenna for different step tread lengths on glass epoxy substrate.

#### 4.1.2. Performance Studies with Step Tread Length Increment

The  $S_{11}$  plots with  $w' = 0.5$  mm,  $0.75$  mm and  $1$  mm are shown in Figure 7. EP6 shows maximum shift of  $\sim 2$  GHz from the designed resonant frequency. Wider step tread length variations ( $w' > \Delta L$ ) yielded a dual band characteristics. The values are tabulated in Table 2.

The measured radiation patterns for  $E$  and  $H$  planes with increment in step tread length are shown in Figures 8(a), (b) and (c), respectively. EP3 shows best directive property with directivity of  $11.34$  dBi. The directivities are tabulated in Table 2.

## 4.2. Results for Step Profile Antenna on Magnetodielectric Substrate

MPA resonating at  $8$  GHz is designed on synthesized  $5\%$  VF nickel ferrite/LDPE substrate, with step riser height and tread length varying in similar fashion as the dielectric substrate is studied.

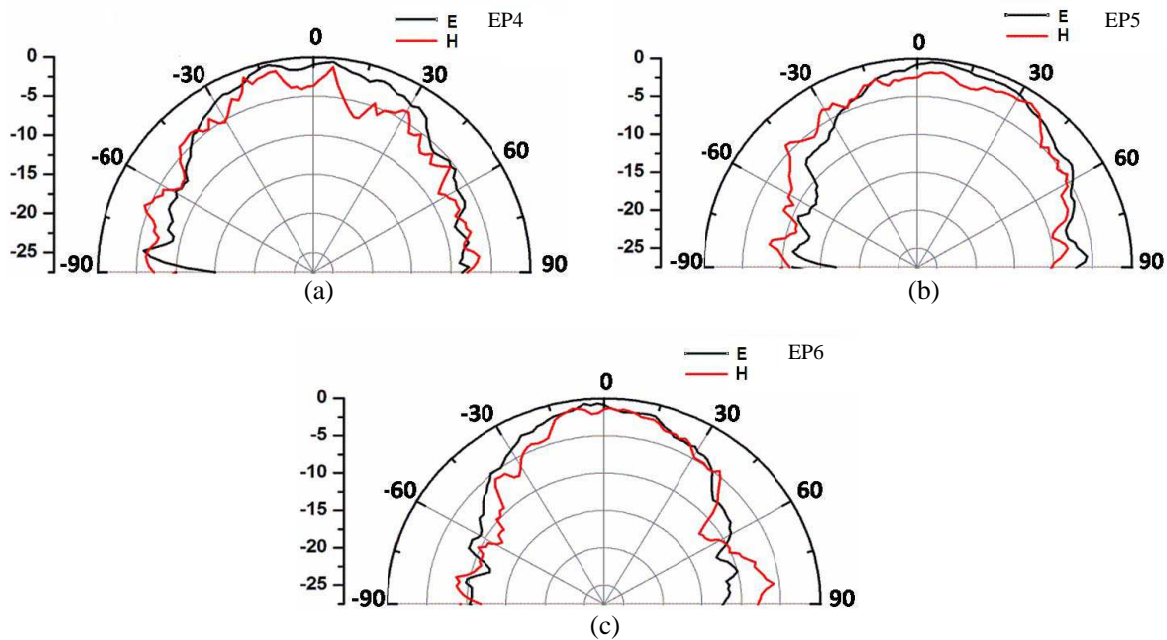


**Figure 8.** (a)  $E$  and  $H$  plane radiation patterns (measured) of EP4 ( $w' = 0.5$  mm) on glass epoxy substrate. (b)  $E$  and  $H$  plane radiation patterns (measured) of EP5 ( $w' = 0.75$  mm) on glass epoxy substrate. (c)  $E$  and  $H$  plane radiation patterns of EP6 (measured) ( $w' = 1$  mm) on glass epoxy substrate.

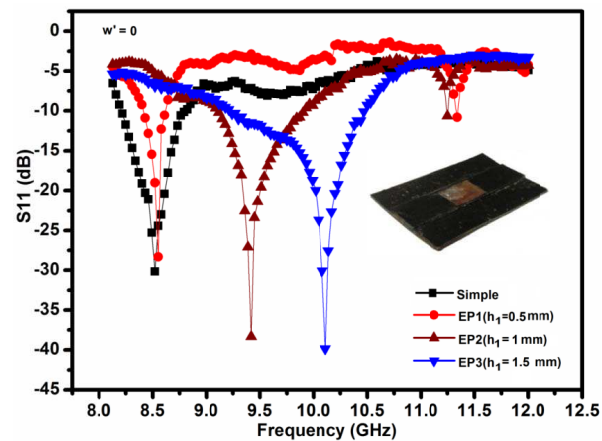


**Figure 9.**  $S_{11}$  (measured) of the step profile antenna for different step riser heights on 5% VF nickel ferrite/LDPE substrate

#### 4.2.1. Performance Study with Step Riser Height

The  $S_{11}$  plots with different step riser heights are shown in Figure 9. The resonant frequency of stepped structure, as compared to planar structure, shifts towards the higher side. An increase in  $S_{11}$  and  $-10$  dB bandwidth is observed as the step riser height increases. EP3 configuration shows a 14.6%  $-10$  dB bandwidth with  $S_{11}$  of  $\sim -40$  dB at 10.25 GHz. The results are tabulated in Table 2.

The measured radiation patterns in both  $E$  and  $H$  planes for  $h_1 = 0.5$  mm, 1 mm and 1.5 mm are shown in Figures 10(a), (b) and (c), respectively. EP3 configuration shows highest directivity of 8.63 dBi. The directivities are tabulated in 2.



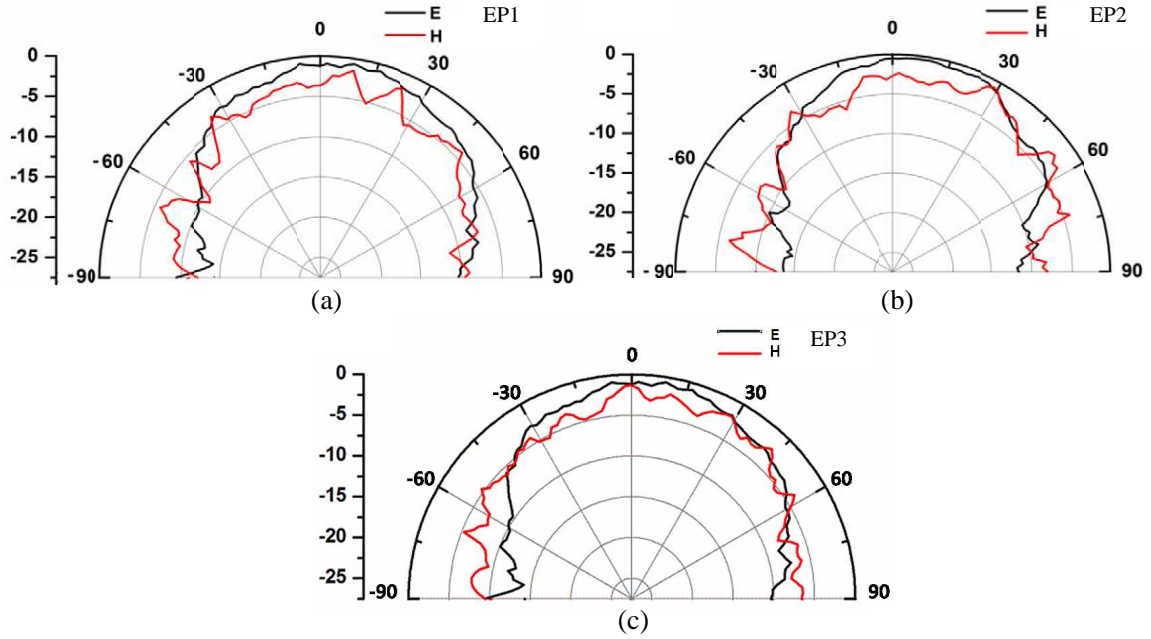


**Figure 10.** (a)  $E$  and  $H$  plane radiation patterns (measured) of EP1 ( $h_1 = 0.5$  mm) on 5% VF nickel ferrite/LDPE substrate. (b)  $E$  and  $H$  plane radiation patterns of EP2 (measured) ( $h_1 = 1$  mm) on 5% VF nickel ferrite/LDPE substrate. (c)  $E$  and  $H$  plane radiation patterns of EP3 (measured) ( $h_1 = 1.5$  mm) on 5% VF nickel ferrite/LDPE substrate.

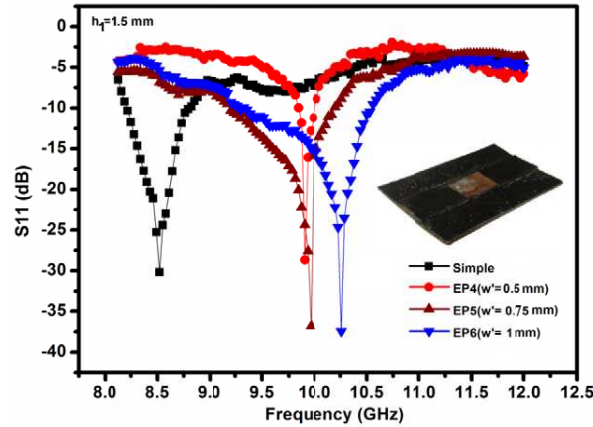


**Figure 11.**  $S_{11}$  (measured) of the step profile antenna for different step tread lengths on 5% VF nickel ferrite/LDPE substrate.

#### 4.2.2. Performance Study with Step Tread Length Variations

The  $S_{11}$  plots with different step tread lengths are shown in Figure 11.  $S_{11}$  and  $-10$  dB bandwidth increase with increase in step tread length,  $w'$ . A shift in resonant frequency is observed from the design frequency in this case too. For EP6,  $S_{11}$  of  $\sim -39$  dB is observed with  $-10$  dB bandwidth of 14%. The results are tabulated in Table 2.

The measured radiation patterns for  $E$  and  $H$  planes for  $w' = 0.5$  mm,  $0.75$  mm and  $1$  mm are shown in Figures 12(a), (b) and (c), respectively. The EP4 configuration shows highest directivity of  $9.21$  dBi. The directivities are tabulated in Table 2.



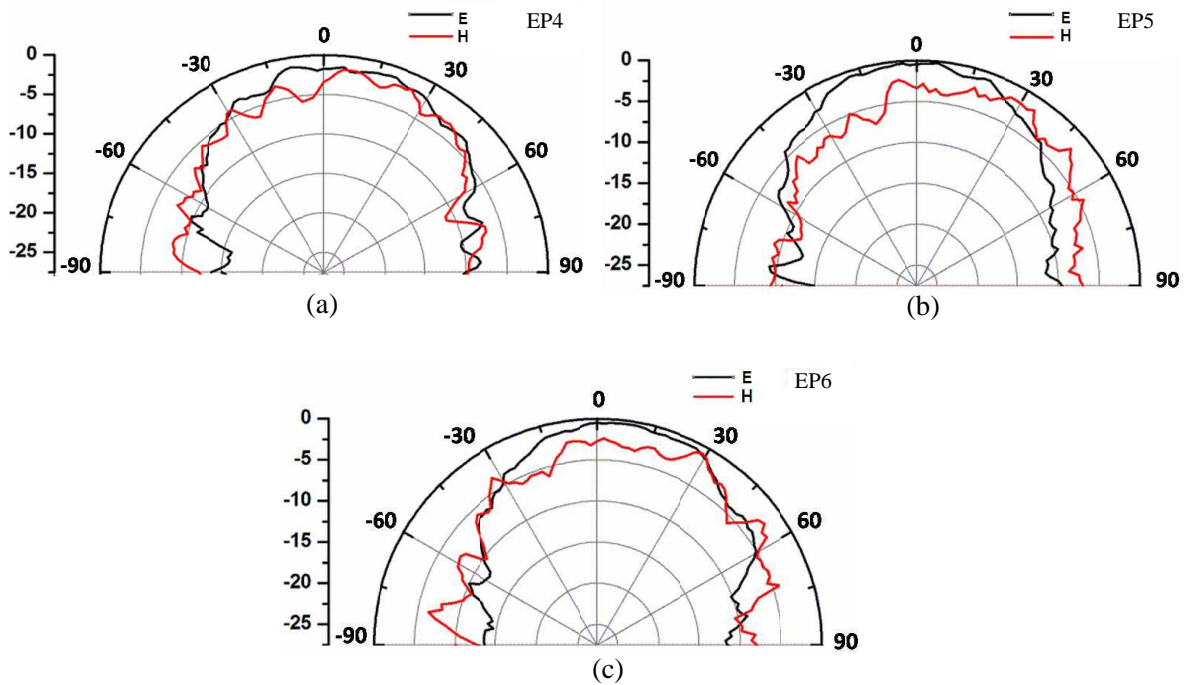


**Figure 12.** (a)  $E$  and  $H$  plane radiation patterns (measured) of EP4 ( $w' = 0.5$  mm) on 5% VF nickel ferrite/LDPE substrate. (b)  $E$  and  $H$  plane radiation patterns (measured) of EP5 ( $w' = 0.75$  mm) on 5% VF nickel ferrite/LDPE substrate. (c)  $E$  and  $H$  plane radiation patterns (measured) of EP6 ( $w' = 1$  mm) on 5% VF nickel ferrite/LDPE substrate.

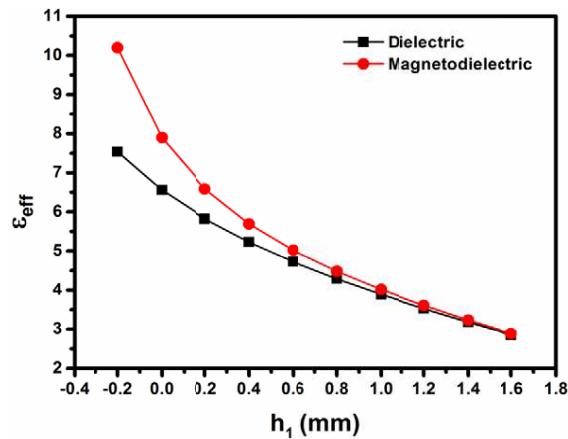


**Figure 13.** Effective permittivity from ECM for different values of  $h_1$  for glass epoxy and 5% VF nickel ferrite/LDPE substrate.

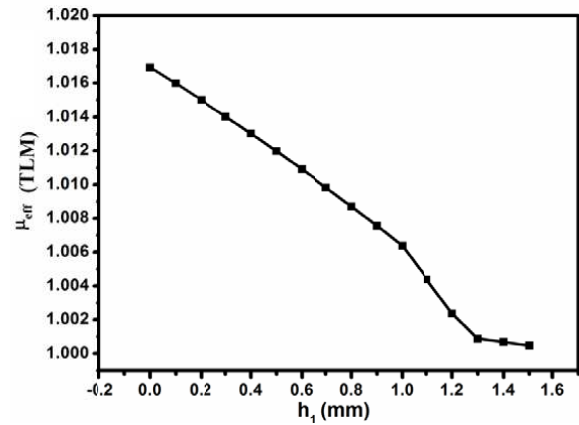


**Figure 14.** Effective permeability from ECM for different values of  $h_1$  for 5% VF nickel ferrite/LDPE substrate.

## 5. DISCUSSIONS

From the equivalent circuit model (ECM) for stepped profile, the effective permittivity,  $\epsilon_{eff}$  and permeability  $\mu_{eff}$  for the magnetodielectric substrate and effective permittivity,  $\epsilon_{eff}$  for the dielectric substrate with step riser height is calculated from Equations (5) and (9). The  $\epsilon_{eff}$  decreases with step riser height and the variation are plotted in Figure 13.

The  $\mu_{eff}$  variations with step riser height are plotted Figure 14. The fields at the radiating edges

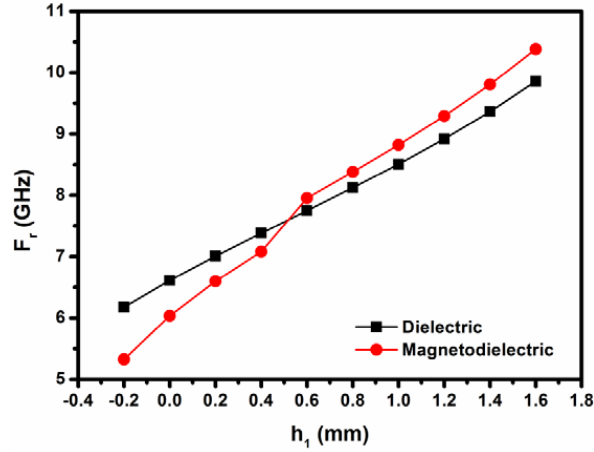


**Figure 15.** Resonant frequency from TLM for different values of  $h_1$  for dielectric and magnetodielectric substrate.

**Table 3.** Difference in resonant frequency from design frequency in ECM and experimental observations.

MPA type	$F_r$ theoretical (GHz)	$F_r$ Experimental (GHz)	$\Delta F_r$ theoretical (GHz)	$\Delta F_r$ Experimental (GHz)
Glass epoxy				
EP1	7.57	8.296	-0.43	0.296
EP2	8.48	9.30	0.48	1.30
EP3	9.6	9.71	1.6	1.71
5% VF nickel ferrite/LDPE				
EP1	8.11	8.5	0.11	0.5
EP2	8.91	9.4	0.91	1.4
EP3	12.11	10.25	4.11	1.25

travel more through air with lower permittivity and permeability than the substrate, as the step riser height increases. This will lead to decrease of effective permittivity and permeability, and hence a decrease is observed with increase in  $h_1$ .

From the  $\varepsilon_{eff}$  and  $\mu_{eff}$  values, resonant frequency,  $F_r$ , of the antenna can be found from

$$F_r = \frac{1}{2(L + \Delta L)\sqrt{\varepsilon_{eff}\mu_{eff}}\sqrt{\varepsilon_0\mu_0}} \quad (10)$$

The plot of  $F_r$  with step riser height is shown in Figure 15. It can be seen that as the height of the substrate decreases in vicinity to the radiation edge,  $F_r$  increases. The results follow the same trend as experimental resonant frequency with increasing  $h_1$ . The shift in resonant frequency from both experimental and ECM as compared to design frequency is also in agreement. The results are tabulated in Table 3.

The measured performance parameter of step profile antenna on 5% VF nano nickel ferrite/LDPE composite and glass epoxy substrate with variation in step profile with different step riser heights and step tread lengths is tabulated in Table 2.

The decrease in effective permittivity of the substrate due step design lowers the surfaces waves [12], hence enhancing the performance. The performance enhancement with increase in  $w'$ , is also observed. The step structures on magnetodielectric substrate are studied under influence of external magnetic bias, but no significant changes are observed, which is in agreement with the results obtained for 5% VF nickel ferrite/LDPE antenna.

As compared to stepped structure fabricated on dielectric glass epoxy substrate, step profile on 5% VF nickel ferrite is shows better performance, as seen from the results in Table 2. Moreover, due to the stepped structure of the substrate, there is volume and hence a weight reduction in the stepped antenna. The % reduced weight of the stepped antenna as compared to that of the planar antenna is shown in Table 4.

**Table 4.** Measured weights of different samples of antennas.

MPA type	Percentage of weight reduced compared to the planar antenna	Percentage of weight reduced compared to the planar antenna
	Glass epoxy	5% VF nickel ferrite/LDPE
Planar	0 %	0%
EP1	18.25%	19.6%
EP2	36.5%	39.3%
EP3	54.75%	58.9%
EP4	52.25%	56.4%
EP5	51%	55.2%
EP6	49.75%	53.9%

## 6. CONCLUSION

Performance study of MPA on dielectric and magnetodielectric substrate in X band by partially removing the substrate along the radiating edge reduces the weight and shows an enhanced  $S_{11}$  parameter,  $-10$  dB bandwidth and directivity as compared to planar substrate antennas. Moreover, multiresonance is observed for some of the samples. The resonant frequency and the shift calculated from the proposed equivalent circuit model for step profile follows in close proximity with the experimental results. The magnetodielectric substrate shows a miniaturization factor of  $n = \sqrt{\mu_r \epsilon_r} = 3.14$ . Thus, bandwidth enhancement along with weight reduction can be done by modifying the substrate structure. The reduction of surface waves due to lowering of effective dielectric constant can reduce the end fire radiation, decreasing interference with devices in proximity to the antenna and may lead to more compact structure.

## REFERENCES

1. Murugan, S. A. S., K. Karthikayan, N. A. Natraj, and C. R. Rathish, "A compact T-fed slotted microstrip antenna for wide band application," *International Journal of Scientific & Technology Research*, Vol. 2, No. 8, 291–294, 2013.
2. Rani, R. and D. Kumar, "Comparative study of T slot & cross slot coupled microstrip patch antenna," *International Journal of Advanced Research in Computer Science and Software Engineering*, Vol. 3, No. 4, 441–445, 2013.
3. Jaafar, H., M. T. Ali, S. Subahri, A. L. Yusof, and M. K. M. Salleh, "Improving gain performance by using air substrate at 5.8 GHz," *International Conference on Computer and Communication Engineering*, 95–98, 2012.
4. Sharma, A., V. K. Dwivedi, and G. Singh, "THz rectangular microstrip antenna design using photonic crystal as Substrate," *PIERS Proceedings*, 161–165, Cambridge, USA, Jul. 2–6, 2008.
5. Jackson, D. R., J. T. Williams, A. K. Bhattacharyya, R. L. Smith, S. J. Buchheit, and S. A. Long, "Microstrip patch designs that do not excite surface waves," *IEEE Transactions on Antennas and Propagation*, Vol. 41, No. 8, 1026–1037, 1993.

6. Papapolymerou, I., R. F. Drayton, and L. P. B. Katehi, "Micromachined patch antennas," *IEEE Transactions on Antennas and Propagation*, Vol. 46, No. 2, 275–283, 1998.
7. Kim, J.-G., H. S. Lee, H.-S. Lee, J.-B. Yoon, and S. Hong, "60-GHz CPW-fed post-supported patch antenna using micromachining technology," *IEEE Microwave and Wireless Components Letters*, Vol. 15, 635–637, 2005.
8. Tzeng, Y.-B., C.-W. Su, and C.-H. Lee, "Study of broadband CP patch antenna with its ground plane having an elevated portion," *Asia Pacific Microwave Conference*, Vol. 4, 2005.
9. Raghava, N. S., A. De, N. Kataria, and S. Chatterjee, "Stacked patch antenna with cross slot electronic band gap structure," *International Journal of Information and Computation Technology*, Vol. 3, No. 5, 1–4, 2013.
10. Yeap, S. B. and Z. N. Chen, "Microstrip patch antennas with enhanced gain by partial substrate removal," *IEEE Transactions on Antennas and Propagation*, Vol. 58, No. 9, 2811–2816, 2010.
11. Borah, K. and N. S. Bhattacharyya, "Magnetodielectric composite with  $\text{NiFe}_2\text{O}_4$  inclusions as substrates for microstrip antennas," *IEEE Transactions on Dielectrics and Electrical Insulation*, Vol. 19, No. 5, 1825–1832, 2012.
12. Kim, Y., G.-Y. Lee, and S. Nam, "Efficiency enhancement of microstrip antenna by elevating radiating edges of patch," *Electronics Letters*, Vol. 39, No. 19, 1363–1364, 2003.
13. Hu, F. G., J. Song, and T. Kamgaing, "Modelling of multilayered media using effective medium theory," *IEEE 19th Conference on Electrical Performance of Electronic Packaging and Systems (EPEPS)*, 225–228, 2010.
14. Edwards, T. C., *Foundations of Microstrip Circuit Design*, John Wiley & Sons, UK, 1981.
15. Hu, F. G., J. Song, and T. Kamgaing, "Modelling of multilayered media using effective medium theory," *IEEE 19th Conference on Electrical Performance of Electronic Packaging and Systems (EPEPS)*, 225–228, 2010.